Journal of Microscopy, Vol. 230, Pt 1 2008, pp. 134–142
Received 30 July 2007; accepted 30 October 2007

Upgrading a microscope with a spiral phase plate

C. MAURER, A. JESACHER, S. FÜRHAPTER, S. BERNET & M. RITSCH-MARTE
Division for Biomedical Physics, Innsbruck Medical University Müllerstr, 44, A-6020 Innsbruck, Austria

Key words. Fourier filtering, phase reconstruction, spiral phase plate.

Summary

We present the implementation of a spiral phase plate in a standard bright-field microscope to enhance the contrast of phase and amplitude samples. The method can be employed in all types of microscopy where standard phase contrast methods are applicable, for example, in bright-field transmission or reflection microscopy using an illumination source with partial spatial coherence. The spiral phase filter is placed into an accessible Fourier plane of the imaging path of the microscope. It is shown that this produces not only a strong contrast enhancement but in theory also improves the spatial resolution of the microscope for white light. A series of different set-ups for transmissive or reflective samples, including epi-illumination, are presented to demonstrate the practical range of applications of this contrasting method. A minute shift of the spiral phase plate out of the centre results in relief-like images that are similar to those obtained by differential interference contrast microscopy. A series of such relief-like images can be numerically processed to obtain quantitative phase and amplitude information of the sample.

Introduction

Many biological samples are pure-phase samples, and therefore show only small contrast in conventional bright-field microscopy. Phase contrast and differential interference contrast (DIC) solve this problem, but both methods require serious modifications of the microscope. For phase contrast microscopy one needs a modified objective, and for DIC two Wollaston prisms, one in front of the condenser and the other behind the objective. Khonina *et al.* (1992), Jaroszewicz & Kolodziejezyk (1993) and Swartzlander (2001) have proposed a spiral phase plate as a Fourier filter to enhance the contrast of amplitude samples. In 2000, the principle was demonstrated by Davis *et al.* for an amplitude object. Later, Fürhapter *et al.* (2005) used a spatial light modulator (SLM) in a microscopy set-up to implement the spiral phase filter and to study its properties in detail. They demonstrated orientation-independent contrast enhancement of both amplitude and phase gradients in a sample. It was also shown that a slightly modified filter function produces relief-like images that visualize the phase landscape of a sample, similar to a DIC image. Furthermore, it was demonstrated (Jesacher *et al.*, 2005; Bernet *et al.*, 2006) how the relief effect can be used to quantitatively calculate the phase profile of a sample, similar to a DIC technique with a rotating sample that was demonstrated by Shribak & Inoue (2006).

In this work, we show how to implement spiral phase microscopy by simply placing a commercially available spiral filter plate into an accessible plane in the optical pathway of the microscope. The spiral phase plate acts as an on-axis diffractive optical element, and not as an off-axis hologram as in our previous experiments. Rotschild *et al.* (2004) have produced an adjustable spiral phase plate by deforming a cracked plexiglas plate. A method for a photo-lithographical fabrication of such an on-axis spiral phase plate is explained in Oemrawsingh *et al.* (2004). In our case, a commercially obtainable spiral phase plate (RPC Photonics, Rochester) was used. It consists of a spiral phase profile with a helicity of $m = 1$ that is imprinted on a photopolymer film coated on a 9×9 mm^2 quartz glass plate. The 'stair step' of the spiral phase plate has an optical thickness of 650 nm, corresponding to the desired 2π step for a light wavelength of 650 nm. This spiral phase plate is placed in an accessible Fourier plane of the optical path of a standard microscope (Zeiss, Axiovert 135, Carl Zeiss AG, Oberkochen, Germany), without any other modification. For the microscope illumination in transmission mode, it was possible to use the standard bright-field condenser, however, with an almost closed illumination aperture to generate the necessary *spatial* coherence. Spatial coherence in this case means that the illumination light (without a sample in the optical pathway) focusses at a sufficiently small spot in the Fourier plane where the spiral phase plate is centred. The size of this spot as compared to the spatial extension of the Fourier image of the sample in the same Fourier plane determines

Correspondence to: Christian Maurer. e-mail: christian.maurer@i-med.ac.at

the minimal size of the sample structures that appear with an intensified edge contrast in the image.

Although our spiral phase plate was tailored for an imaging wavelength of 650 nm, it turned out that even for white light illumination, good edge contrast enhancement could be achieved. Even better contrast enhancement and dispersion suppression was achieved by introducing a line filter with a bandwidth of 12.5 nm into the optical path. This turned out to work well, although the filter had a central transmission wavelength of 532 nm.

In the following the basic concept of spiral phase filtering will be explained. It will be shown that the theoretically achievable spatial resolution of a spiral phase-filtered image can exceed that of standard bright-field image for the case of (temporally) incoherent illumination. The following section presents some experimental results for spiral phase filtering in different experimental set-ups. These include an inverted transmissive design, a reflective design and an epi-illumination set-up. The article concludes with the demonstration how a quantitative reconstruction of the optical thickness profile of a biological sample can be obtained. This uses the fact that image filtering with a spiral phase plate corresponds to a common path interferometer.

Resolution criteria for spiral phase filters

A spiral phase filter has a complex amplitude transmission function of $e^{i\varphi}$, where φ is the azimuth angle. If it is employed as a Fourier filter, it performs a two-dimensional generalization of the one-dimensional Hilbert transformation (Larkin *et al.*, 2001). For an infinite aperture, this would correspond to a convolution with the point-spread-function (PSF) of an ideal filter, $ie^{i\theta}/(2\pi r^2)$, where r and θ are the polar coordinates measured from the centre of the filter (however, in practice the aperture is limited, thus removing the singularity of the PSF at $r = 0$).

The filter kernel transforms a point of the object plane to a focussed doughnut mode with a helical charge of one in the imaging plane. The phase of the doughnut increases from 0 to 2π in a complete turn. Filtering of an expanded object corresponds to its convolution with such a doughnut kernel and, due to the phase shift of π for opposite radial directions homogeneous areas become dark. In practice, this is due to the fact that the light from homogeneous areas focusses exactly at the central phase singularity of the spiral phase plate. There the light is transformed into an evanescent wave (Roux, 2003), or scattered out of the optical pathway of the microscope. By contrast, phase or amplitude edges within the sample are intensified, due to a re-distribution of light from adjacent regions of destructive interference (i.e. homogeneous areas) to the gradient regions, where constructive interference happens.

Note that the phase of the edges still exhibits values in the range between 0 and 2π around the object contour. Interfering the filtered image with a reference beam results in a shadow-like image, where the phase of the reference beam determines the apparent direction of the shadow. A more detailed explanation of the spiral phase kernel can be found in Fürhapter *et al.* (2007).

To determine the resolution of spiral phase-filtered images, first one has to investigate under which circumstances two adjacent object points can be distinguished in the image. For the case of 'normal' imaging, two criteria are commonly used: the Rayleigh criterion and the Sparrow criterion. In the case of the spiral phase kernel, a comparable criterion has to be found.

The Rayleigh criterion considers the images of two adjacent object points (cyan and green graph) that correspond basically to the point-spread function of the microscope objective. The two points are distinguishable, if the central *maximum* of the diffraction pattern of one point lies beyond the first *minimum* of the other (Fig. 1A). By contrast, the point-spread function of the spiral phase-filtered image corresponds to a focussed doughnut mode, rather than to a focussed spot as in the case of a normal bright-field microscope. Since the centre of the doughnut mode is determined by the location of its central dark spot, a comparable definition for a spiral kernel could be in the following: Two object points can be resolved, if the central *minimum* of one focussed doughnut ring lies beyond the first *maximum* (i.e. the 'ring') of the other (see Fig. 1B). According to this definition, the spiral filtered images reach a higher resolution than bright-field images recorded with the same numerical aperture: The minimal distance for two points to be distinguishable decreases by 36%.

According to the Sparrow criterion, two image points are resolved, when their total intensity distribution along their connecting line has a local *minimum* (red graph) between the two points. Since the position of a spiral filtered point is "tagged" by the central minimum of the spiral kernel, two vortex filtered points are analogously resolved, when there is a local intensity *maximum* between them. The right side of Fig. 1 sketches the Sparrow criterion applied to the point-spread function of a circular aperture and to that of a spiral kernel. In the case of temporally incoherent light, the resolution of spiral phase-filtered images is again improved by 20%.

Adapting the microscope

Figure 2 shows how the spiral phase plate can be implemented within an inverted microscope (Zeiss, Axiovert 135). The horizontal front port of our microscope offers an accessible Fourier plane, where all optical components such as the tubus lens (TL), the imaging lens L_1 and the prism can remain untouched. The Fourier plane is located around 3 cm behind the imaging lens L_1. The spiral phase plate is positioned with a three-dimensionally controllable micrometre stage. The images are recorded with a DVC 1394 camera (DVC Company, Austin, Texas). The bright-field image can be simultaneously

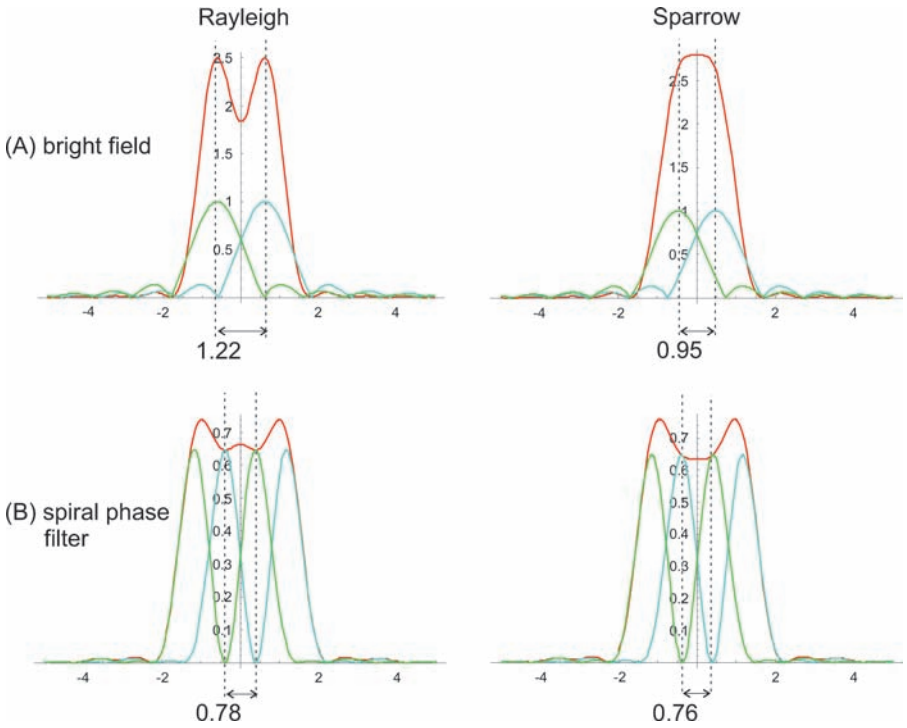

Fig. 1. Resolution of the spiral phase filter calculated with a scalar, paraxial theory. The left graphs show the resolution distance when the Rayleigh criterion is applied, the right ones for the Sparrow criterion. In the case of the Rayleigh criterion, two points (green and cyan) are distinguishable, when their angle displacement is larger than 1.22 λ/D for a bright-field image, and 0.78 λ/D for spiral phase filtering. When the Sparrow criterion is used, the minimal angle for bright-field microscopy is 0.95 λ/D and 0.76 λ/D with a spiral phase filter. λ is the wavelength and D the diameter of the imaging aperture. The red line delineates the total intensity.

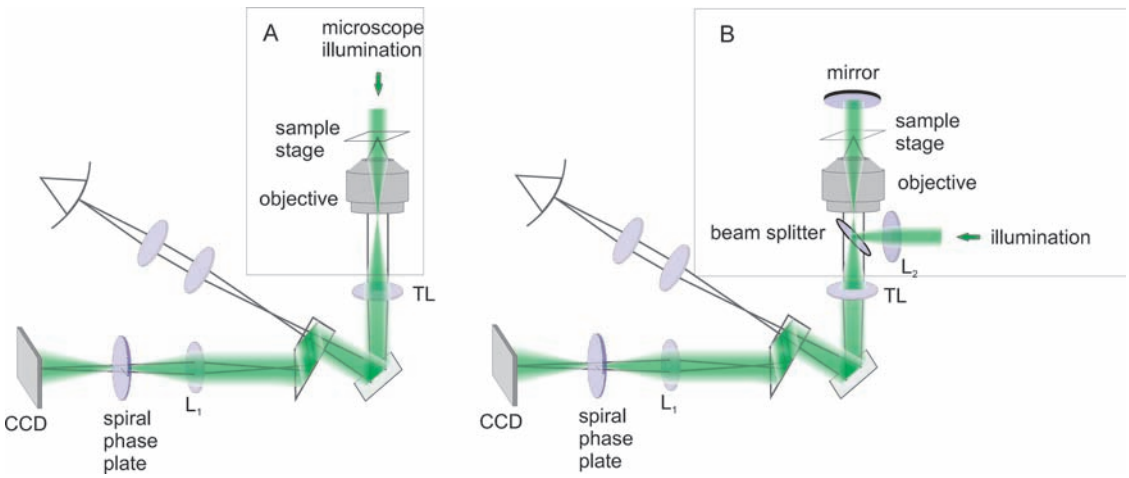

Fig. 2. The light path modifications used for spiral filtering. Graphic A shows the set-up for transmissive probes, set-up B is for reflective probes with epi-illumination. The optical path after the tubus lens (TL $f = 160$ mm) is the same for both set-ups. The spiral phase plate is inserted into the Fourier plane of the horizontal front port of the microscope. The distance from the tubus lens to the CCD is approximately 370 mm, and the lens L_1 has a focal length of 50 mm. In the case of a transmissive probe (set-up A) the illumination aperture has to be chosen rather small (NA = 0.03 in our experiments). In the case of a reflective set-up (B), a beam splitter and an additional lens L_2 ($f = 100$ mm) have to be placed into the optical path of the microscope. The lens L_2 focuses the input beam to the Fourier plane of the objective. The collimated light leaving the objective is either reflected by the probe or, in the case of a transmissive sample, reflected by an additional mirror. Lens L_2 focuses the illumination beam to a spot size of 100 μm to the focal plane of the objective.

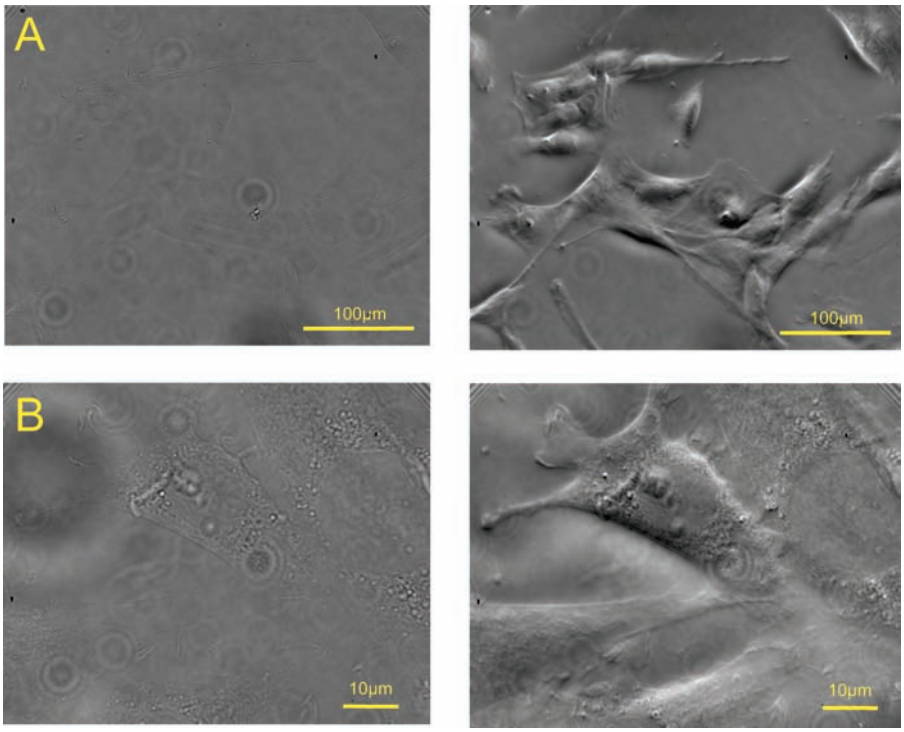

Fig. 3. The images show fibroblast cells in line A as viewed with a 20× air objective, in line B recorded with a 100× oil immersions objective. The images at the left side show the bright-field images, whereas at the right are the corresponding spiral phase-filtered images. The centre of the spiral phase plate is placed 50 µm away from the optical axis. The recording time of the spiral phase-filtered images is only half as long as that of the bright-field images.

viewed through the normal imaging path. The box (A) illustrates how the illumination of transmissive probes is achieved. The normal microscope illumination condenser was used, with a strongly reduced opening of the illumination aperture (NA = 0.03).

For reflective targets, like semi-conductor surfaces, the illumination can be modified (see box B). Now the illumination light is coupled in through the epi-illumination port of the microscope using a 45/55 pellicle beam splitter. A lens L_2 (f = 100 mm) focusses the beam of collimated light to the rear focal plane of the objective, such that the probe is illuminated with a plane wave. The remaining divergence of the illumination light depends on the used objective, and corresponds to a numerical aperture of NA = 0.0031 for the 10× objective, and NA = 0.02 for 63× air objective. The back-reflected image wave then passes again the 45/55 beam-splitter, and its transmitted part is spiral phase-filtered as before.

The same principle can also be applied for the imaging of transmissive samples with epi-illumination through the objective. This is sometimes useful, if there are spatial restrictions in the experimental set-up that prevent the use of a standard illumination system. For this purpose, the sample is again illuminated with a plane wave that comes through the objective. However, since the sample is transmissive, the illumination light is now back-reflected to the imaging path of the microscope by a plane mirror at a position behind the sample. On a first glance, the method seems to suffer from the double pass of the light wave through the sample, but it was found that there is almost no disturbance.

Figure 3 shows a comparison between bright-field and spiral phase–filtered fibroblast cells, recorded with the imaging set-up of Fig. 2A. The left images are the bright-field images, whereas the right images are recorded with the spiral phase filter. The spiral phase plate was slightly displaced out of the centre (by about 50 µm), in order to obtain the relief effect. All of the demonstrated images are presented without any post-processing. The examples of the first line (A) were imaged with a 20× air objective (NA = 0.45), whereas the cells in the lower line (B) were recorded with a 100× oil immersion objective (NA = 1.3). The examples demonstrate a strong contrast enhancement of the spiral phase method as compared to bright-field images. Note that the exposure time that used the full dynamic range of the CCD for the spiral phase-filtered image is only one half of that for the bright-field images. This demonstrates an edge intensity amplification that is due to a coherent re-distribution of light from homogeneous areas to phase edges (Fürhapter *et al.*, 2005).

To demonstrate the applicability of spiral phase filtering to *reflective* samples, Fig. 4 compares a section of a semi-conductor surface recorded as a bright-field image (right column) and a spiral phase-filtered image (left column), respectively. The set-up for recording these images corresponded to that in Fig. 2B.

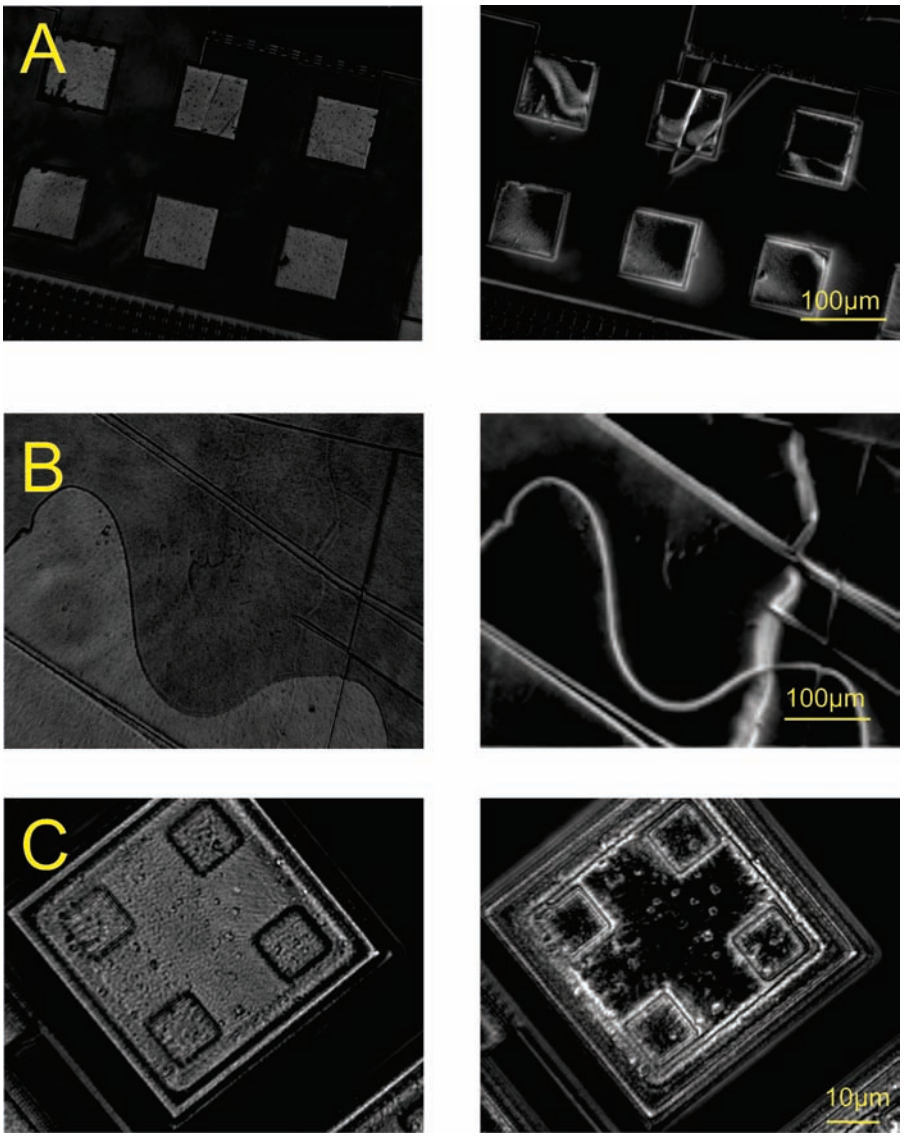

Fig. 4. Section of the surface of a semi-conductor device. The images in line A and B are recorded with a 10× objective, the images in line C are viewed with a 63× air objective. The left column shows the bright-field image, the spiral phase-filtered images are shown on the right side. The spiral phase plate is centred at the optical axis of the microscope.

The images in lines A and B (upper two rows of Fig. 4) were recorded with a 10× air objective (NA = 0.25), whereas the images in line C (lowest row) were recorded with a 63× air objective (NA = 0.95). The contrast of the bright-field images at the left side of all rows is due to the spatial distribution of the sample reflection coefficient. However, the spiral phase-filtered images at the right side contain much more information about the sample. They clearly display a variety of sample structures that are not visible in the bright-field images. Note for example, the 'buckled' vertical line in the right part of Fig. 4B, which is almost invisible in the bright-field image. Note that a good quality of the spiral phase-filtered image is even obtained with a microscope objective with a high numerical aperture (NA = 0.95), despite the fact that such a high NA introduces vectorial effects. This demonstrates the robustness of the SPP method with respect to polarization effects.

As already mentioned, the same set-up that was just used for imaging reflective samples with epi-illumination, can be also used for imaging transmissive samples. For that purpose, an additional mirror is mounted above the transmissive sample reflecting the illumination beam back through the sample and the objective. Figure 5 shows a cheek cell observed with four different settings. The sample was viewed with a 60× oil objective (NA = 1.25). To get sufficient illumination light for recording the weakly back-reflecting phase samples, now a laser was used as illumination source (frequency doubled Nd:Yag laser at a wavelength of 532 nm with a coherence length of 1m). Images A and C are recorded without the

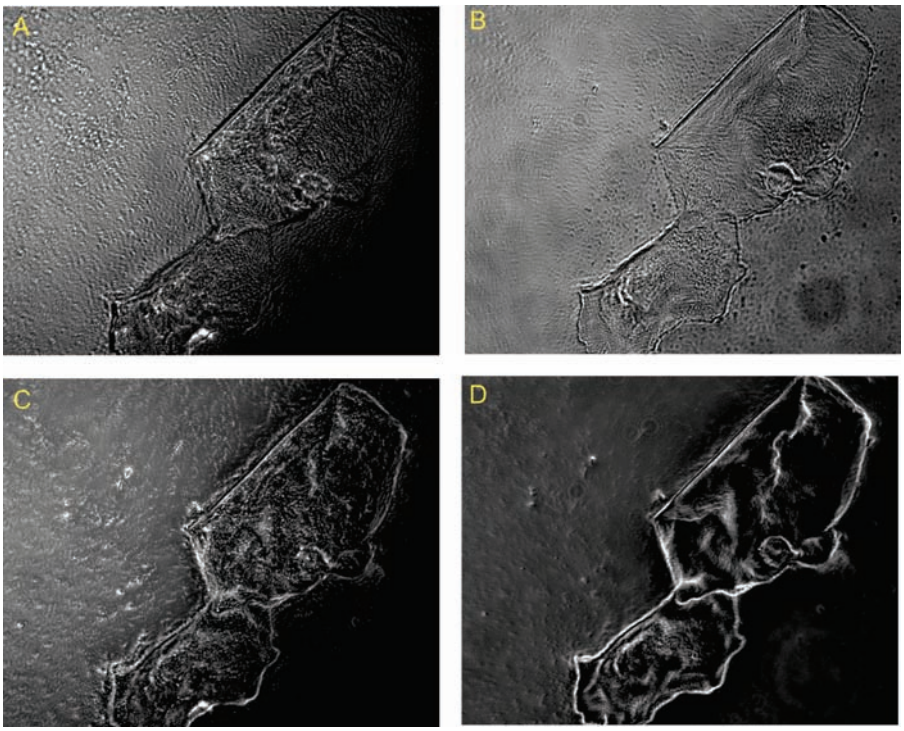

Fig. 5. Images A–D show two cheek cells illuminated with an epi-fluorescence set-up. The sample was imaged with an 60× oil objective using green laser light (532 nm). Images A and C are the backscattered light without and with the spiral phase plate in the Fourier plane, respectively. Images B and D are the forward scattered images, where illumination is achieved by a mirror approximately 1 cm above the object. Image B is the bright-field image, and image D shows the spiral phase-filtered image.

back-reflection mirror, and thus correspond to surface reflection images, whereas the images B and D are recorded with a back-reflecting mirror located 1 cm behind the sample. A and B are unfiltered images, whereas C and D are spiral phase filtered.

Image A presents a standard reflection image of the cheek cells. The image is formed from back-scattered light, giving the cell the appearance of a brighter structure against a dark background. The spiral phase-filtered reflection image (C) already shows an isotropic edge enhancement. However, since the amount of back-scattered light—and thus the "reference wave"— is only small, both images, (A) and (C), are afflicted by a noisy background.

To avoid this, a back-reflection mirror was installed at a position 1 cm behind the sample, providing an intense wave for transmission microscopy, in order to get a better signal-to-noise ratio. The incident plane illumination wave now first passes through the sample, where most of the illumination is just transmitted as a 'zero-order component' without being disturbed, whereas a small fraction of the light is scattered by the sample. The transmitted light is then reflected by the mirror, and passes again through the sample. Afterwards, the image wave is spiral phase filtered and recorded by a camera as before. Thus the plane illumination wave component that has passed a first time through the sample, and is then reflected by the mirror now acts as a plane illumination wave in set-up (Fig. 2B). The small fraction of the light that is scattered by the sample contributes to a small 'background', that is, of light that cannot be spiral phase filtered, but that forms a weak bright-field image of the sample that is superposed on the spiral phase-filtered image. Note that due to the presence of the mirror, in fact two images of the sample are recorded by the set-up, that is, the object itself, and its mirror image. However, the effective distance from the mirror image to the microscope objective is much larger than the depth of focus of the objective, such that the mirror-imaged component is completely out of focus and only contributes as a small homogeneous background. Since the light has already gone through the sample once, on the way back from the mirror the sample is now illuminated by partially coherent light. However, it turns out that this effect is small and does not diminish the quality of the image.

Figure 5B shows an image that is recorded with the mirror set-up, but without spiral phase filtering. Note that it is about 20× brighter than its corresponding reflection image A. For recording image D the spiral phase plate was introduced and centred in the plane where the back-reflected epi-illumination light had a focus. The result shows that for the chosen position of the mirror the spiral phase-filtered transmission image of the cell is, indeed, very similar to the images obtained with the normal transmission set-up of Fig. 2A. A possible application of

such a set-up could be Fourier filtering in an epi-fluorescence microscope. The fluorescence light of the sample is not only temporally but also spatially incoherent. In this case, the spiral phase filter does not produce the effects of edge amplification or homogeneous area attenuation. Therefore, the fluorescence image appears as almost unperturbed (a small difference to a standard fluorescence image is, however, expected in the case of a very high resolution, due to the different PSF of the spiral phase filter). With the mirror above the probe, the transmission image recorded with the fluorescence excitation source is combined with the fluorescence image. Because the excitation light is collimated, it can be used to obtain a spiral phase-filtered image with resulting edge enhancement. Thus, as a result, one obtains a fluorescence image of a sample that is superposed by a spiral phase contrast image, showing both, sample contours and fluorescence, at the same time.

In Jesacher *et al.* (2006), it was shown that the information about the phase landscape of a sample can be retrieved from a series of spiral filtered 'shadow-effect' images, with changing directions of the apparent shadow. This idea uses the fact that the spiral phase filtering set-up corresponds to a self-referenced interferometer, where the spiral phase-filtered image is coherently combined with a plane light wave that corresponds to the zero-order Fourier component of the image wave. These experiments were performed with a SLM acting as the spiral phase filter. The SLM was programmed to display spiral phase structures with a small unmodulated (i.e. 'flat') spherical area in the centre, thus transmitting an undisturbed zero-order wave component that served as a reference wave.

In this work, a manufactured spiral phase plate is used, thus re-programming of the spiral phase structure is not possible. Nevertheless, it can be used for a similar method to reconstruct the phase landscape of a sample. In our case, an 'undisturbed' zero-order component of the image wave is transmitted through the spiral phase plate, if the centre of the plate is slightly shifted with respect to the position of the illumination light focus. In the image plane, this zero-order wave component is superposed again with the other Fourier components of the image that are spiral filtered, thus producing a 'shadow-image' that is actually an interferogram of the spiral phase-filtered sample, with the zero-order plane wave acting as a reference wave. The direction of the displacement (i.e. up, down, left, right) of the spiral phase plate centre from the illumination beam focus determines a phase offset

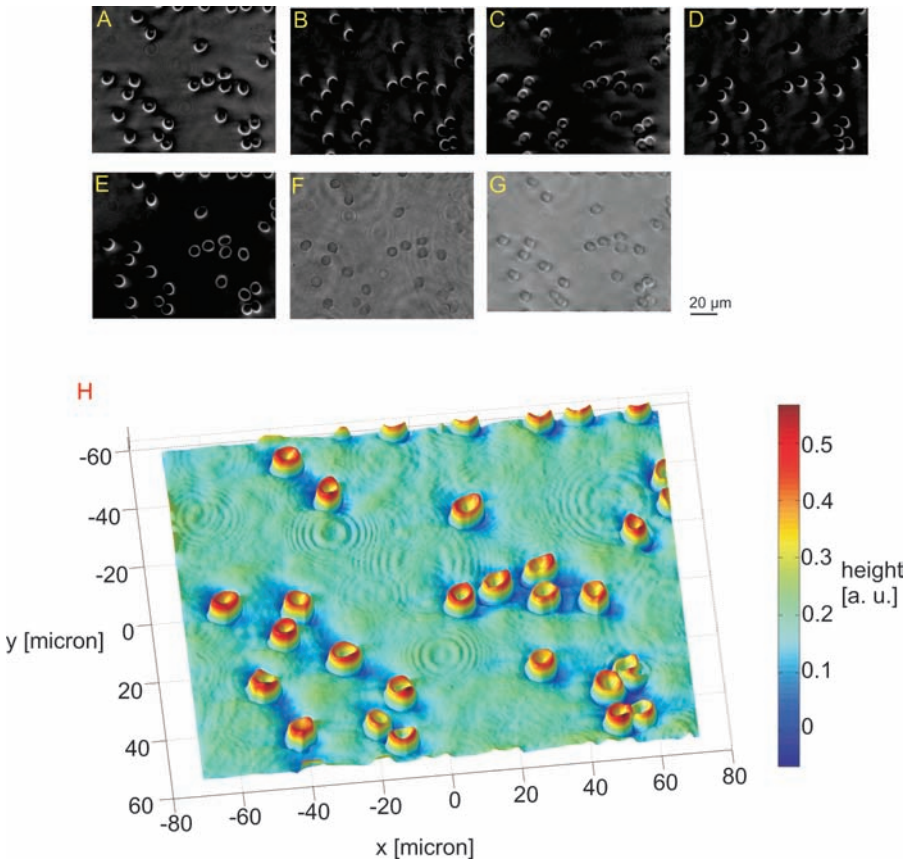

Fig. 6. Images A–D show the spiral phase-filtered images of erythrocytes when the filter is shifted slightly off centre by about 50 µm. A perfectly aligned spiral phase filter isotropically enhances the edges of the cells, as is shown in image E. Image F and G are the recorded and the reconstructed bright-field images of the sample, respectively. Image H shows the reconstructed phase of the sample.

acquired by the zero-order light with respect to the remaining, spiral phase-filtered wave. Thus, the resulting interferogram produces different apparent 'shadow directions' in the image, depending on the displacement direction of the spiral phase plate.

A result of images obtained with different spiral phase plate displacement directions is shown in Fig. 6: Human erythrocytes are imaged with a 60× oil immersion objective (NA = 1.25). The cells were diluted with physiological saline solution and sandwiched between two glass plates. Figures 6(A–D) comprise a series of shadow images. The corresponding phase shifts were $\pi/2$, π, $3\pi/2$ or 2π, adjusted by moving the filter to the right, up, to the left and down, respectively. For a small displacement, the outer Fourier components that arise from steep edges or fine details of the sample, still acquire the spiral phase shift. However, Fourier components in the close vicinity of the zero-order Fourier component see the same phase as the zero order. This means that flat regions of the sample are not properly spiral phase filtered and that a size-dependent underestimation of structures by occur (larger structures appear shallower than smaller ones). Further displacement of the filter leads to a decrease of the spiral filtering effect, until it is completely lost and the bright-field image (F) is obtained. Thus there is an optimum displacement, which in our particular set-up was experimentally determined to be 50 μm, and which was used to record the images in Fig. 6(A–D). For comparison, the resulting image for an exactly centred spiral phase filter is displayed in E. As expected, it shows an isotropic edge enhancement. Images G and H represent the bright-field intensity and phase of the sample, as calculated from the images in Fig. 6(A–D), using the method described in Bernet *et al.* (2006). The surface plot in image H represents the optical thickness of the sample structures and clearly exhibits the toroidal shape of the erythrocytes. However, the exact quantitative data for the optical thickness depend, as described earlier, on the details of the set-up, like the collimation of the illumination beam and the shift distance of the spiral phase plate. Therefore, a preliminary calibration of the set-up has to be performed, if quantitative data are required.

Conclusion

In this work, we have studied the phase contrast enhancement that can be obtained by the insertion of a commercially available spiral phase plate in a standard bright-field microscope. In contrast to previous investigations of spiral phase filtering in microscopy, now the spiral phase element is just a 'refractive' hardware optical component, acting as an on-axis spatial Fourier filter, and not a 'diffractive' structure like an off-axis hologram that was used in earlier work, and there displayed at a spatial light modulator. Our on-axis refractive implementation has the advantage that there is no dispersion introduced by off-axis diffractive components, and that the field of view is not restricted by a limited diffraction angle. It turned out that, although a spiral phase filter is designed for a certain wavelength, strong contrast enhancement can even be achieved using white light illumination from a standard microscope condenser with a narrow illumination aperture. If the spiral phase plate is exactly centred in the Fourier plane with respect to the optical axis, there results an isotropic edge enhancement, which is, for example, desirable for computer-controlled cell recognition or for particle counting. By contrast, a filter displacement results in shadow-like images resembling DIC images, with a characteristic relief-like impression of the sample phase profile. The shadow direction is adjustable by selecting the direction in which the spiral phase plate is de-centred. This effect can be used to record a series of four shadow images with different apparent shadow directions that can be numerically processed to get a quantitative determination of the phase and amplitude profile of a sample. The presented method is one of the cheapest possibilities to upgrade a standard microscope with a highly efficient phase contrasting method, since the only modification of the microscope consists in the insertion of a single spiral phase plate that can be rather low prized, if produced in larger quantities.

Acknowledgment

This work was supported by the Austrian Academy of Sciences (DOC Scholarship for A.J.) and by the Austrian Science Foundation (FWF) Project No. P18051-N02 and Project No. P19582.

References

Bernet, S., Jesacher, A., Fürhapter, S., Maurer, C. & Ritsch-Marte, M. (2006) Quantitative imaging of complex samples by spiral phase contrast microscopy. *Opt. Express* **14**, 3792–3805.

Davis, J.A., McNamara, D.E., Cottrell, D.M. & Campos, J. (2000) Image processing with the radial Hilbert transform: theory and experiments. *Opt. Lett.* **25**, 99–101.

Fürhapter, S., Jesacher, A., Maurer, C., Bernet, S. & Ritsch-Marte, M. (2007) Spiral phase microscopy. *Advances in Imaging and Electron Physics* (ed. by P.W. Hawkes), Vol. **146**, 1–56, Academic Press.

Fürhapter, S., Jesacher, A., Bernet, S. & Ritsch-Marte, M. (2005) Spiral phase contrast imaging in microscopy. *Opt. Exp.* **13**, 689–694.

Larkin, K.G., Bone, D.J. & Oldfield, M.A. (2001) Natural demodulation of two-dimensional fringe patterns. I. General background of the spiral phase quadrature transform. *J. Opt. Soc. Am. A.* **18**, 1862–1870.

Jaroszewicz, Z. & Kolodziejczyk, A. (1993) Zone plates performing generalized Hankel transformation and their metrological application. *Opt. Commun.* **102**, 391–396.

Jesacher, A., Fürhapter, S., Bernet, S. & Ritsch-Marte, M. (2005) Shadow effects in spiral phase contrast microscopy. *Phys. Rev. Lett.* **94**, 233902.

Jesacher, A., Fürhapter, S., Bernet, S. & Ritsch-Marte, M. (2006) Spiral interferogram analysis. *J. Opt. Soc. Am. A* **23**, 1400–1409.

Khonina, S.N., Kotlyar, V.V., Shinkaryev, M.V., Soifer, V.A. & Uspleniev, G.V. (1992) The phase rotor filter. *J. Mod. Opt.* **39**, 1147–1154.

Oemrawsingh, S.S.R., Houwelingen, van J.A.W., Eliel, E.R., Woerdman, J.P., Verstegen, E.J.K., Kloosterboer, J.G. & Hooft, 'tG.W. (2004) Production and characterization of spiral phase plates for optical wavelengths. *Appl. Opt.* **43**, 688–694.

Roux, F.S. (2003) Optical vortex density limitation. *Opt. Commun.* **223**, 31–37.

Rotschild, C., Zommer, S., Moed, S., Hershcovitz, O. & Lipson, G.S. (2004) Adjustable spiral phase plate. *Appl. Opt.* **43**, 2397–2399.

Shribak, M. & Inoue, S. (2006) Orientation-independent differential interference contrast microscopy. *Appl. Opt.* **45**, 30460–30469.

Swartzlander, G.A. Jr. (2001) Peering into darkness with a vortex spatial filter. *Opt. Lett.* **26**, 497–499.

